3. Sandrock D, Merino MJ, Norton JA, Neumann RD. Parathyroid imaging by Tc/Tl scintigraphy. *Eur J Nucl Med* 1990;16:607–613.
4. Coakley AJ, Kettle AG, Wels CP, O'Doherty MJ, Collins REC. Tc-99m sestamibi: a new agent for parathyroid imaging. *Nucl Med Commun* 1989;10:791–794.
5. Taillefer R, Boucher Y, Potvin C, Lambert R. Detection and localization of parathyroid adenomas in patients with hyperparathyroidism using a single radionuclide imaging procedure with technetium-99m-sestamibi (double-phase study). *J Nucl Med* 1992;33:1801–1807.
6. O'Doherty MJ, Kettle AG, Wells P, Collins REC, Coakley AJ. Parathyroid imaging with technetium-99m-sestamibi: preoperative localization and tissue uptake studies. *J Nucl Med* 1992;33:313–318.
7. Geatti O, Shapiro B, Orsolon PG, et al. Localization of parathyroid enlargement: experience with technetium-99m methoxyisobutylisonitrile and thallium-201 scintigraphy, ultrasonography and computed tomography. *Eur J Nucl Med* 1994;21:17–22.
8. Lee VS, Wilkinson RH, Leight GS, Coogan AC, Coleman RE. Hyperparathyroidism in high-risk surgical patients: evaluation with double-phase technetium-99m sestamibi imaging. *Radiology* 1995;197:627–633.
9. Ishibashi M, Nishida H, Kumabe T, et al. Tc-99m tetrofosmin: a new diagnostic tracer for parathyroid imaging. *Clin Nucl Med* 1995;20:902–905.
10. Nishihara S, Tsuneyoshi M. Papillary cystic tumours of the pancreas: an analysis by nuclear morphometry. *Virchows Archiv A Pathol Pathol Anat* 1993;422:213–217.
11. Moolenaar W, Heslinga JM, Arndt JW, Velde CJH, Parwels EKJ, Valentijn RM. Tl-201 — Tc-99m subtraction scintigraphy in secondary hyperparathyroidism of chronic renal failure. *Nephrol Dial Transplant* 1988;2:166–168.
12. Kessler M, Avila JM, Renoult E, Mathieu P. Reoperation for secondary hyperparathyroidism in chronic renal failure. *Nephrol Dial Transplant* 1991;6:176–179.
13. Adalet I, Hawkins T, Clark F, Wilkinson R. Thallium–technetium subtraction scintigraphy in secondary hyperparathyroidism. *Eur J Nucl Med* 1994;21:509–513.
14. Rossitch JC, Cowan RJ, Ellis MB, Griffith RF. Technetium-99m sestamibi for detection of parathyroid adenoma. Comparison of single and dual tracer imaging. *Clin Nucl Med* 1995;20:220–221.
15. Highley B, Smith FW, Smith T, et al. Technetium-99m-1,2-bis[bis(2-ethoxy-ethyl)phosmino]ethane: human biodistribution, dosimetry and safety of a new myocardial perfusion imaging agent. *J Nucl Med* 1993;34:30–38.
16. Gooding CAW. Sonography of the thyroid and parathyroid. *Radiol Clin North Am* 1993;116:974–989.
17. Rodriguez JM, Tezelman S, Spierstein AE, et al. Localization procedures in patients with persistent or recurrent hyperparathyroidism. *Arch Surg* 1994;129:870–875.
18. Piga M, Bolasco P, Satta L, et al. Double-phase parathyroid technetium-99m-MIBI scintigraphy to identify functional autonomy in secondary hyperparathyroidism. *J Nucl Med* 1996;37:565–569.
19. Sandrock D, Merino MJ, Norton JA, Neumann RD. Ultrastructural histology correlates with results of thallium-201/technetium-99m parathyroid subtraction scintigraphy. *J Nucl Med* 1993;34:24–29.
20. Chiu ML, Kronange RJ, Piwnica-Worms D. Effect of mitochondrial and plasma-membrane potentials on accumulation of hexakis (2-methoxyisobutylisonitrile) technetium in cultured mouse fibroblasts. *J Nucl Med* 1990;31:1646–1653.
21. Crane P, Laliberte R, Heminway S, Thoolen M, Oriandi C. Effect of mitochondrial viability and metabolism on technetium-99m-sestamibi myocardial retention. *Eur J Nucl Med* 1993;20:20–25.
22. Benard F, Lefebvre B, Beuvon F, Langlois MF, Bisson G. Rapid washout of technetium-99m-MIBI from a large parathyroid adenoma. *J Nucl Med* 1995;36:241–243.
23. Younes A, Songadele JA, Maublant J, Platts E, Pickett R, Veyre A. Mechanism of uptake of technetium-tetrofosmin. II: uptake into isolated adult rat heart mitochondria. *J Nucl Cardiol* 1995;2:327–333.

Characterizing an Ectopic Secreting Carcinoid with Indium-111-DTPA-D-Phe-Pentetreotide

V. Briganti, M. Mannelli, G. La Cava, A. Peri, U. Meldolesi, R. Masi and A. Pupi
Department of Nuclear Medicine, Azienda Hospital Careggi–Florence; and Department of Clinical Pathophysiology, University of Florence, Florence, Italy

This report describes a technique that increases the specificity of ^{111}In-pentetreotide as evaluated in a patient with ectopic Cushing syndrome. **Methods:** Two separate SPECT studies were performed with different pharmacologic protocols, both including treatment with cold octreotide. The imaging protocol provides acquisitions at 4 and 24 hr after injection. The quantitative approach was based on the ROI activity (manually designed) of an area of pathological lung uptake (ROI-T) versus background (ROI-NT). Histological, histochemical and specific mRNA measurements confirmed the presence of an SSR2 receptor carcinoid in the lung. **Results:** The time course of ROI-T/ROI-NT is a linear increase between 4 and 24 hr. Washout with cold octreotide diminished the ROI-T activity content and the saturation protocol increased ROI-T/ROI-NT, confirming the specific nature of the uptake. **Conclusion:** Displacement and saturation protocols in ^{111}In-pentetreotide imaging demonstrated the specificity of tumor binding.

Key Words: somatostatin receptors; indium-111-pentetreotide; octreotide; ectopic Cushing syndrome

J Nucl Med 1997; 38:711–714

The use of ^{111}In-DTPA-D-Phe-pentetreotide in the scintigraphic diagnosis of well-differentiated neuroendocrine tumors has been reported (*1,2*), but a model-based approach and/or the use of pharmacological interventions have not been used to increase the specificity of the imaging procedure, which is hampered by false-positive results due to unspecified binding in the tumor.

We have tried to characterize the in vivo distribution of ^{111}In-pentetreotide with a combined kinetic uptake study and the use of displacement doses of nonlabeled octreotide, and we have evaluated the results of this novel approach with a biological model of the in vivo behavior of labeled pentetreotide as a receptor ligand. This report describes an individual patient where the results of the study had a significant influence in clinical management.

CASE REPORT

A 31-yr-old woman was admitted to the endocrinology unit at the University of Florence for suspected Cushing's syndrome. The presence of the syndrome was confirmed by high levels of urinary free cortisol, plasma cortisol and plasma ACTH, absence of circadian rhythm in cortisol secretion, absence of cortisol and ACTH response to insulin-induced hypoglycemia and absence of suppression in plasma cortisol and ACTH after 2 mg of oral dexamethasone.

An ACTH-dependent Cushing's syndrome due to an ectopic secretion was suspected because plasma cortisol and ACTH were not suppressed after administration of 8 mg oral dexamethasone and did not increase after 100 μg intravenous human CRF.

MRI of the pituitary showed a slight bulging of the superior profile of the gland, which was considered a possible indirect sign of the presence of a pituitary microadenoma. However, petrosal venous sampling on both sides failed to demonstrate any ACTH gradient before and after stimulation with CRF (Table 1). An abdominal CT scan showed normal adrenal glands. Plasma ACTH was not suppressed by the administration of 100 μg intravenous octreotide. A second multiple venous sampling along the main venous tree (from the superior vena cava to the iliac veins) was performed and again no ACTH gradient was found (Table 2).

Chest MRI and a second abdominal CT scan, performed in an attempt to reveal the ectopic source of ACTH, failed to show significant findings. Therefore, despite the lack of ACTH suppres-

TABLE 1
ACTH Petrosal Venous Sampling Before and After CRF Stimulation

ACTH	Unit	Results	Time
Superior vena cava	ng/liter	133	0 hr
Interior vena cava	ng/liter	126	0 hr
Peripheries	ng/liter	119	0 hr
		121	+3 hr
		106	+5 hr
		120	+10 hr
Right jugular vein	ng/liter	132	0 hr
		126	Postinjection
Left jugular vein	ng/liter	127	0 hr
		128	Postinjection
Right sinus	ng/liter	122	0 hr
		132	+3 hr
		127	+5 hr
		123	+10 hr
Left sinus	ng/liter	126	0 hr
		116	+3 hr
		122	+5 hr
		128	+10 hr

sion after acute octreotide administration, a series of scintigraphic studies with labeled pentetreotide was performed. These studies demonstrated the presence of an intense uptake region in the anterior lower portion of the right lung. A pulmonary lesion, less than 2 cm in diameter, was confirmed by a selective CT scan (Fig. 1).

During surgery, a 1.5-cm nodule was found. Histological examination revealed the presence of a carcinoid tumor that was intensely positive for ACTH at immunocytology. The presence of SSR2 in the neoplastic tissue was confirmed by the detection of SSR2 mRNA by RT-PCR and Southern blot analysis (Fig. 2).

After surgery, the patient's plasma ACTH and cortisol concentrations fell to undetectable levels and it was necessary to provide a short course of corticosteroid replacement therapy.

SPECT Acquisition Protocol

All SPECT studies were performed with a single-head rotating camera in 64 frames (45 sec each). The matrix dimension was 64 × 64 pixels. Reconstruction was performed with filtered backprojection (Butterworth filter 0.25 cutoff, order 10). ROIs were manually extracted on the transaxial slices delineating the area with pathologic uptake in the right lung (ROI_T) and a symmetrical region with

TABLE 2
ACTH Multiple Venous Sampling and Baseline Levels of Plasma ACTH, Testosterone, DHEA-S and Cortisol

Withdrawal seat	Values (μg/liter)
Left brachicephalic trunk	204
Right jugular vein	227
Superior vena cava (origin)	222
Superior vena cava (right suprabrach.)	222
Superior vena cava (distal vs. atrium)	221
Right atrium	218
Inferior vena cava (D10)	230
Inferior vena cava (D11-D12)	180
Inferior vena cava (L1-L2)	200
Inferior vena cava (L2-L3)	188
Inferior vena cava (L4)	187

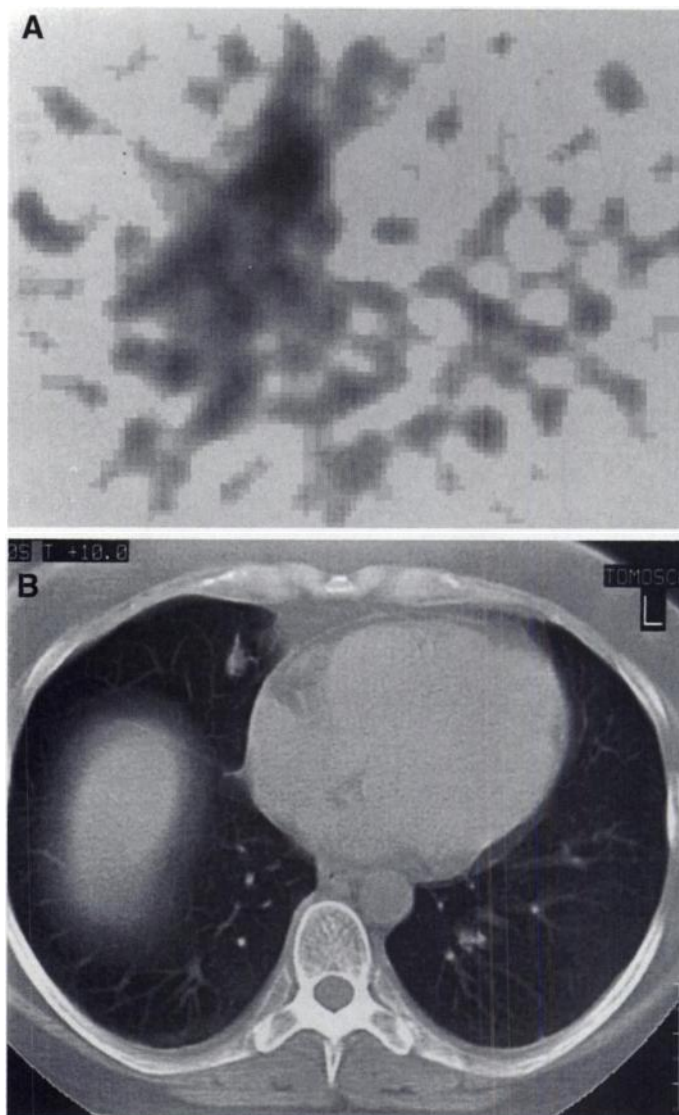| Baseline values			
ACTH	232 μg/liter	DHEA-S	1.92 μg/liter
Testosterone	2.6 nM/liter	Cortisol	464 nM/liter

FIGURE 1. (A) Transaxial SPECT section and (B) corresponding CT slice obtained after administration of ^{111}In-pentetreotide.

normal uptake in the left lung (ROI_{NT}). Count content was normalized for ROI pixel number.

Study Protocol

The patient was studied on two separate sessions. First, a wash-out study, consisted of the injection of the tracer (111 MBq ^{111}In-pentetreotide) and the acquisition of two SPECT studies at 4
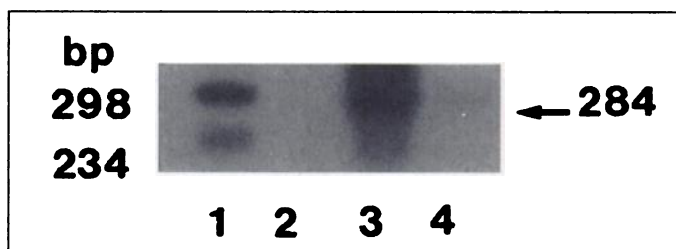

FIGURE 2. Total RNAs extracted from the neoplastic tissue or from a human neuroblastoma cell line (CHP 404, which overexpresses SSR2) were subjected to RT-PCR using oligonucleotide primers derived from sequence of sst_2 cDNA. A chemically modified nucleotide (digoxigenin-11-dUTP) was included in the PCR mixture. The PCR products were electrophoresed in agarose gel, blotted into a nylon membrane and detected by an immune-enzymatic procedure (3). Lane 1: DNA mole weight marker VI; lane 2: negative control (no RNA); lane 3: CHP 404; lane 4: lung ACTH-secreting tumor. The arrow indicates the bp PCR product, specific for sst_2.
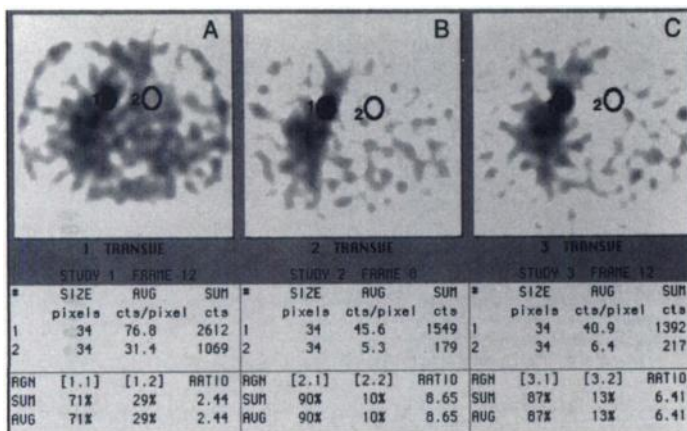
FIGURE 3. Three octreoscan transaxial SPECT sections of the patient executed at (A) 4, (B) 24 and (C) 26 hr after tracer administration. The third SPECT study (C) was executed after a 2-hr single-step displacement with cold octreotide. Imaging of transaxial SPECT sections with manual ROIs (1 as T and 2 as NT) extracted. Bottom: Size and count activity (as count/pixel and total counts) of ROI 1 and ROI 2 of every transaxial SPECT section and ROI_T/ROI_{NT} at 4, 24 and 26 hr. The time course of the T/NT ratio shows a straight increased between (A) 4 and (B) 24 hr. (C) In contrast, administration of cold octreotide abruptly diminishes the ROI_T activity content and the T/NT ratio.

the ROI_T/ROI_{NT} ratio should be stable or decrease between 4 and 24 hr.

The pharmacologic interventions with cold octreotide were performed to further assess the specific nature of the uptake in ROI_T.

RESULTS

The time course of the ratio ROI_T/ROI_{NT} is reported in Figure 3, and it shows a straight increase between 4 and 24 hr. The washout with octreotide abruptly diminished the ROI_T activity content, thus confirming the specific nature of the uptake in ROI_T. Interestingly, the steady-state study showed an increase of the ROI_T/ROI_{NT} ratio, which was explained by the different affinity for the ligand of the SSR2 receptor of the tumor and of the normal tissue (Fig. 4). The overexpression of SSR2 receptor in the tumor was confirmed ex vivo by immunocytochemistry and specific m-RNA measurement (PCR).

DISCUSSION

Scintigraphic localization of tumor with ^{111}In-pentetreotide depends on the presence of somatostatin binding sites in the tumor at a higher density and affinity than that of the surrounding normal tissues. Consequently, SPECT with pentetreotide can be considered an in vivo method to biologically characterize tumors originating from the neural crest. Unfortunately, the tumor activity also can be due to nonspecific uptake because of modification of tumor vasculature and extravascular spaces and contents. Results are often difficult to interpret (4).

This report describes an evaluation of the SPECT scan with pentetreotide based on analysis of the biological model of SSR2 receptor content of the tumor and normal tissue. The pharmacologic interventions that have been performed are a method of identifying the model and validating the results.

Indeed, pharmacologic interventions are a common practice in studying brain receptors, and both displacement (5) and saturation (6,7) protocols have been proposed. We applied a similar approach to the study with pentetreotide and demonstrated the specificity of tumor binding on the basis of increased ROI ratios, between 4 and 24 hr. In accordance, tumor activity exhibited a significant reduction after injection of a displacement dose of cold octreotide.

The ex vivo demonstration of a significant band of the mRNA for somatostatin receptors in the tumor finally confirmed the correctness of the diagnosis.
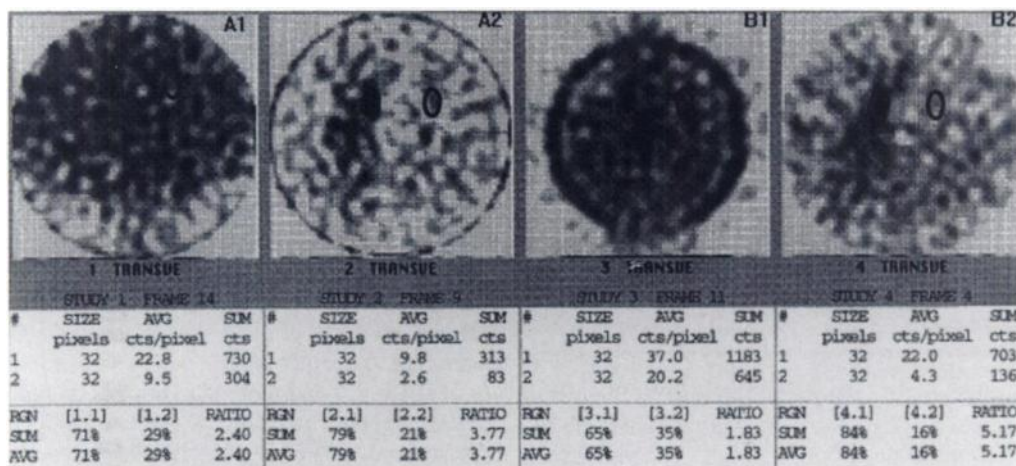
and 24 hr after injection. Subsequently, a slow intravenous infusion of 0.5 mg of octreotide in 100 ml of saline was given. A SPECT was acquired 2 hr later.

For the steady-state study, performed 2 wk later, the patient received 0.3 mg per day of subcutaneous octreotide and an intravenous dose of 0.2 mg (intravenous bolus injection) 4 days before SPECT was performed. SPECT acquisitions were performed 4 and 24 hr after tracer injection.

Data Evaluation

The results of the first phase of the washout study were evaluated under the following three assumptions: the activity in ROI_{NT} is due to tracer binding to the SSR2 receptor of normal tissue; the quantity of SSR2 receptor in normal tissue is constant; and the activity retained in ROI_T and ROI_{NT} at 4 and 24 hr is due only to receptor-bound tracer.

Under the above assumptions, if the activity in ROI_T is due to the overexpression of SSR2 receptor, the ROI_T/ROI_{NT} ratio should increase between the 4-hr and 24-hr SPECT images. On the contrary, if the activity in ROI_T at 4 hr is due to nonspecific uptake,

FIGURE 4. Four pentetreotide transaxial SPECT slices of the patient. Left sections show transaxial slices at (A1) 4 hr and (A2) 24 hr of the baseline study. The right sections show transaxial slices at (B1) 4 hr and (B2) 24 hr of the steady-state study. Top: Imaging of transaxial SPECT sections with manual ROIs (1 as T and 2 as NT) extracted. Bottom: Size and count activity, as count/pixel and total counts, of every transaxial SPECT section and ROI_T/ROI_{NT} at 4 and 24 hr for baseline and steady-state studies. The time course of T/NT ratio shows an unexpected increase in the steady-state study.

The most interesting result is that the same information also could be obtained with the model-based interpretation of the SPECT scan, thus avoiding the cumbersome and expensive pharmacologic protocol described above. Indeed, assuming the receptor model is used, the simple observation of the temporal behavior to the ROI_T/ROI_{NT} ratio gives strong evidence that tumor uptake was specific.

Therefore, we suggest pentetreotide can be extended beyond its use as a tumor detection agent to that of a tumor characterizing agent, which increases the clinical importance of the scintigraphic data and may provide direction for therapeutic management. This aim probably will be best fulfilled by true quantitative approaches (8), but the simplicity of the method we propose can represent a reasonable trade-off in clinical management. Future developments of SSR2 receptor tracers, labeled with more favorable isotopes (9) and with high-resolution SPECT instrumentation, can further increase the value of the biological in vivo characterization of SSR2-expressing tumors.

REFERENCES

1. Krenning EP, Kwekkeboom DJ, Bakker WH, et al. Somatostatin receptor scintigraphy with ^{111}In-DTPA-D-Phe- and ^{123}I-Tyr-octreotide. The Rotterdam experience with more than 1000 patients. Eur J Nucl Med 1993;8:715–731.
2. Lamberts SWJ, Krenning EP, Reubi JC, et al. The role of sandostatin and its analogs in the diagnosis and treatment of tumors. Endocr Rev 1991;4:450–482.
3. Peri A, Cordellea-Niele E, Miele L, Mukherje AB. Tissue-specific expression of the gene coding for human clara cell 10-kD protein: a phosphoerpase A_2-inhibitory protein. J Clin Invest 1993;92:2099–2109.
4. Maini CL, Tofani A, Venturo I, et al. Somatostatin receptor imaging in small cell lung cancer using ^{111}In-DTPA-D-Phe-octreotide: a preliminary study. Nucl Med Commun 1993;14:962–968.
5. Innis RB, Al-Tikriti MS, Zoghbi SS, et al. SPECT imaging of the benzodiazepine receptors: feasibility of in vivo potency measurement from stepwise displacement curves. J Nucl Med 1991;9:1754–1761.
6. Morlein SM, Welch MS. Application of SPECT to the in vivo measurement of benzodiazepine potency. J Nucl Med 1991;9:1762–1763.
7. Lassen NA. Neuroreceptor quantitation in vivo by the steady-state principle using constant infusion or bolus injection of radioactive tracers. J Cereb Blood Flow Metab 1992;5:709–716.
8. Eckelman WC. The application of receptor theory to receptor-binding and enzyme-binding oncologic radiopharmaceuticals. Nucl Med Biol 1994;5:759–769.
9. Bakker WH, Krenning EP, Reubi JC, et al. In vivo application of [111In-DTPA-D-Phe]-octreotide for detection of somatostatin receptor-positive tumors in rats. Life Sci 1991;49:1593–1601.

Influence of Chemotherapy on FDG Uptake by Human Cancer Xenografts in Nude Mice

Takashi Yoshioka, Hiromu Takahashi, Hirosuke Oikawa, Syunichi Maeda, Tatuo Ido, Takashi Akaizawa, Hiroshi Fukuda and Ryunosuke Kanamaru

Department of Clinical Oncology, Nuclear Medicine and Radiology, Institute of Development, Aging and Cancer and Cyclotron and Radioisotope Center, Tohoku University, Sendai, Japan

This study evaluated the use of PET with ^{18}F-2-deoxy-2-fluoro-D-glucose (^{18}F-FDG) for monitoring chemotherapy effects, using a human cancer xenograft (poorly differentiated human gastric cancer) in vivo model. **Methods:** Tumor ^{18}F-FDG uptakes and sizes were measured after administrating mitomycin (MMC), cisplatin (CDDP) and adriamycin (ADR) to xenograft-bearing nude mice and compared with ^{18}F-FDG tumor uptake and tumor size in a non-therapy group. The correlation between the uptake and size was also assessed. **Results:** The largest reduction in tumor size after chemotherapy occurred in the MMC administered group, followed by the CDDP case, with no reduction in the ADR group as compared to the controls. Fluorine-18-FDG tumor uptake after chemotherapy was also decreased in the MMC and CDDP groups, in that order, but not in the ADR case. With MMC and CDDP, size reduction became significant on Days 8 or 11, whereas ^{18}F-FDG tumor uptake had already been decreased on Days 3 or 7. **Conclusion:** Fluorine-18-FDG uptake decreases in parallel to the efficacy of anticancer agents and correlates with subsequent morphologic changes. We conclude that ^{18}F-FDG PET tumor images are indeed useful for monitoring the effects of cancer chemotherapy.

Key Words: fluorine-18-FDG; human cancer xenograft; PET; chemotherapy

J Nucl Med 1997; 38:714–717

With cancer chemotherapy, it is important to choose the most effective chemotherapeutic agents for individual patients. There have been several attempts to develop in vitro (1–6) and in vivo

(7,8) systems that would predict the response of a tumor, in an individual patient, to a particular chemotherapeutic agent, but the results have been far from satisfactory. In clinical practice, the chemotherapist chooses chemotherapeutic agents on the basis of his experience and by monitoring morphological changes of tumors by physical examination, radiograph studies, endoscopy, CT, US or MRI, in a continuous decision-making process.

The development of PET has made it possible to study the metabolism of cancer tissues. The positron-labeled compound ^{18}F-2-deoxy-2-fluoro-D-glucose (^{18}F-FDG) is widely used in PET as a tracer for glucose metabolism (9) because it is phosphorylated by hexokinase but essentially cannot be further metabolized, becoming preferentially trapped in the cells (10). As enhanced glycolysis is one of the best-documented characteristics of malignant tumors (11), ^{18}F-FDG PET has been used for successful imaging of various kinds of human neoplasms (12–19).

Theoretically, ^{18}F-FDG PET should also be suitable for follow-up after cancer treatment, since its uptake relates to the number of viable tumor cells (20). The response of tumors to chemotherapy might, therefore, be recordable earlier and more exactly in terms of ^{18}F-FDG uptake than from morphological changes. Several clinical studies using ^{18}F-FDG have been performed to evaluate therapeutic response in malignant tumors (14–17, 21–24) and there also have been reports of experimental studies concerned with the relationship between treatment efficacy and ^{18}F-FDG uptake (25,26). However, detailed experimental in vivo studies on the correlation between morphologic alterations and ^{18}F-FDG uptake in tumors caused by chemotherapy have been lacking.

In this study we compared the relationship between tumor